Nonlinear Speed Control for PMSM System Using Sliding-Mode Control and Disturbance Compensation Techniques

Xiaoguang Zhang, Lizhi Sun, *Senior Member, IEEE*, Ke Zhao, and Li Sun, *Member, IEEE*

***Abstract*—In order to optimize the speed-control performance of the permanent-magnet synchronous motor (PMSM) system with different disturbances and uncertainties, a nonlinear speed-control algorithm for the PMSM servo systems using sliding-mode control and disturbance compensation techniques is developed in this paper. First, a sliding-mode control method based on one novel sliding-mode reaching law (SMRL) is presented. This SMRL can dynamically adapt to the variations of the controlled system, which allows chattering reduction on control input while maintaining high tracking performance of the controller. Then, an extended sliding-mode disturbance observer is proposed to estimate lumped uncertainties directly, to compensate strong disturbances and achieve high servo precisions. Simulation and experimental results both show the validity of the proposed control approach.**

***Index Terms*—Disturbance observer, permanent-magnet synchronous motor (PMSM), Sliding-mode control (SMC), sliding-mode reaching law (SMRL).**

I. Introduction

In THE permanent-magnet synchronous motor (PMSM) control system, the classical proportional integral (PI) control technique is still popular due to its simple implementation [1]. However, in a practical PMSM system, there are large quantities of the disturbances and uncertainties, which may come internally or externally, e.g., unmodeled dynamics, parameter variation, friction force, and load disturbances. It will be very difficult to limit these disturbances rapidly if adopting linear control methods like PI control algorithm [20].

Therefore, many nonlinear control methods have been adopted to improve the control performances in systems with different disturbances and uncertainties, e.g., robust control [4], [5], sliding-mode control (SMC) [6], [7], [10], [16], adaptive control [8], backstepping control [9], predictive control [11], intelligent control [13], [14], and so on. In these nonlinear control methods, SMC method is well known for its invariant properties to certain internal parameter variations and external disturbances, which can guarantee perfect tracking performance despite parameters or model uncertainties. It has been successfully applied in many fields [15], [16]. In [6], the fuzzy sliding-mode approach was applied to a six-phase induction machine. In [7], a hybrid terminal sliding-mode observer was proposed based on the nonsingular terminal sliding mode and the high-order sliding mode for the rotor position and speed estimation in one PMSM control system. In [17], the performance of a sliding-mode controller was studied using a hybrid controller applied to induction motors via sampled closed representations. The results were very conclusive regarding the effectiveness of the sliding-mode approach. A neuron-fuzzy sliding-mode controller applied to induction machine can also be found in [15].

However, the robustness of SMC can only be guaranteed by the selection of large control gains, while the large gains will lead to the well-known chattering phenomenon, which can excite high-frequency dynamics. Thus, some approaches have been proposed to overcome the chattering, such as continuation control, high-order sliding-mode method [16], complementary sliding-mode method [18], and reaching law method [2], [3], [12], [19]. The reaching law approach deals directly with the reaching process, since chattering is caused by the nonideal reaching at the end of the reaching phase. In [3], authors presented some reaching laws, which can restrain chattering by decreasing gain or making the discontinuous gain a function of sliding-mode surface. In [12], a novel exponential reaching law was presented to design the speed- and current-integrated controller. To suppress chattering problem, system variable was used in this reaching law. However, in the aforementioned reaching laws, the discontinuous gain rapidly decreases because of variation of the functions of the sliding surface, thus reducing the robustness of the controller near the sliding surface and also increasing the reaching time.

In order to solve the aforementioned problems, a novel reaching law, which is based on the choice of an exponential term that adapts to the variations of the sliding-mode surface and system states, is proposed in this paper. This reaching law is able to deal with the chattering/reaching time dilemma. Based on this reaching law, a sliding-mode speed controller of PMSM is developed. Then, to further improve the disturbance rejection performance of SMC method, extended sliding-mode disturbance observer (ESMDO) is proposed, and the estimated system disturbance is considered as the feedforward compensation part to compensate sliding-mode speed controller. Thus, a composite control method combining an SMC part and a feedforward compensation part based on ESMDO, called SMC+ESMDO method, is developed. Finally, the effectiveness of the proposed control approach was verified by simulation and experimental results.

Manuscript received October 3, 2011; revised November 14, 2011, March 11, 2012, and May 14, 2012; accepted June 16, 2012. Date of current version October 12, 2012. Recommended for publication by Associate Editor K. M. Ralph.

The authors are with the Harbin Institute of Technology, Harbin 150001, China (e-mail: zhangxg123456789@163.com; lzsun@hit.edu.cn; zhk_mail2002@yahoo.com.cn; motor611@sina.com).

Color versions of one or more of the figures in this paper are available online at http://ieeexplore.ieee.org.

Digital Object Identifier 10.1109/TPEL.2012.2206610

II. PRELIMINARIES

In this section, some preliminaries are introduced, including PMSM models and basic SMC design with sliding-mode reaching law (SMRL) method, to facilitate the proposal of the new methods.

A. PMSM Model

One PMSM model in the rotor *d–q* coordinates can be expressed as follows [20]:

$$\begin{aligned} T_e &= 1.5p\psi_a i_q \\ T_e - T_L &= \frac{J}{p}\dot{\omega} + B\omega \\ u_d &= ri_d - \omega L i_q + L\dot{i}_d \\ u_q &= ri_q + \omega L i_d + \omega\psi_a + L\dot{i}_q \end{aligned} \tag{1}$$

where u_d and u_q represent *d* and *q* axes stator voltages, respectively; i_d and i_q are *d* and *q* axes currents, respectively; *L* is stator inductance; *r* is stator resistance; T_e is electrical magnetic torque; T_L is load torque; *p* is number of pole pairs; ψ_a is flux linkage of permanent magnets; ω is electrical angular velocity; *B* is viscous friction coefficient; *J* is rotational inertia.

B. SMC Design With Reaching Law Method

Compared with other nonlinear control methods, SMC is more insensitive to internal parameter variations and external disturbance once the system trajectory reaches and stays on the sliding surface. However, how to design the SMC controller to reduce chattering is crucial, which motivates our researches for a new reaching law introduced in the next section. A complete study of SMRL theory can be found in [3]. In this section, the basic SMC design method is introduced briefly. In general, SMC design can be divided into two steps, the first step is to choose the sliding-mode surface, and the next step is to design the control input such that the system trajectory is forced toward the sliding-mode surface, which ensures the system to satisfy the sliding-mode reaching condition that is expressed as follows:

$$s \cdot \dot{s} < 0 \tag{2}$$

where *s* is the sliding-mode surface.

The following second-order nonlinear model is generally used to describe the SMC system adopting one reaching law method:

$$\begin{cases} \dot{x}_1 = x_2 \\ \dot{x}_2 = f(x) + g(x) + b(x)u \end{cases} \tag{3}$$

where $x = [x_1, x_2]^T$ is system state, $g(x)$ represents the system disturbances, and $b(x)$ is not zero.

The concrete steps include the following. First, the typical sliding-mode surface is chosen as follows:

$$s_1 = cx_1 + x_2. \tag{4}$$

Such sliding-mode surface can guarantee the asymptotic stability of the sliding mode, and the asymptotic rate of convergence is in direct relation with the value of *c*. Next, the control input *u* should be designed in such a way that the sliding-mode reaching condition (inequality (2)) is met. Thus, equal reaching law is typically chosen as follows:

$$\dot{s}_1 = -k_1 \cdot \mathrm{sgn}(s_1). \tag{5}$$

Substituting (4) into (5) yields

$$c\dot{x}_1 + \dot{x}_2 = -k_1 \cdot \mathrm{sgn}(s_1). \tag{6}$$

Next, substituting (3) into (6) yields

$$cx_2 + f(x) + g(x) + b(x) \cdot u = -k_1 \cdot \mathrm{sgn}(s_1). \tag{7}$$

Then, according to (7), the control input *u* can be easily expressed as

$$u = -b^{-1}(x)[cx_2 + f(x) + g(x) + k_1 \cdot \mathrm{sgn}(s_1)]. \tag{8}$$

Here, it can be found that the discontinuous term $-b^{-1}(x)\, k_1 \cdot \mathrm{sgn}(s_1)$ is contained in the control input, which leads to the occurrence of chattering. And the chattering level is up to the value of k_1 directly.

The time required to reach sliding-mode surface can be derived by integrating (5) with respect to time as follows:

$$t_1 = \frac{|s(0)|}{k_1}. \tag{9}$$

It can be observed that this reaching time can also be regulated by the value of k_1 directly. If the value of k_1 is increased, a faster reaching time and a good robustness can be obtained, but the chattering level on the control input also increases. Thus, in order to solve this dilemma, a novel reaching law is proposed in the next section.

III. DESIGN OF SMC SPEED CONTROLLER

A. Proposed SMRL

The novel SMRL is realized based on the choice of an exponential term that adapts to the variations of the sliding-mode surface and system states. This reaching law is given by

$$\begin{aligned} \dot{s} &= -eq(x_1, s) \cdot \mathrm{sgn}(s), \quad eq(x_1, s) \\ &= \frac{k}{[\varepsilon + (1 + 1/|x_1| - \varepsilon)e^{-\delta|s|}]} \end{aligned} \tag{10}$$

where $k > 0$, $\delta > 0$, and $0 < \varepsilon < 1$. x_1 is the system state.

In this novel reaching law, it can be found that if $|s|$ increases, the *eq*$(x_1.s)$ converges to the value of k/ε that is greater than the value of *k*. This indicates that a faster reaching time can be obtained. On the other hand, if $|s|$ decreases, denominator term of the *eq*$(x_1.s)$ approaches $1 + 1/|x_1|$, then the *eq*$(x_1.s)$ converges to $k|x_1|/(1 + |x_1|)$, in which system state $|x_1|$ gradually decreases to zero under the control input designed in the next section. This indicates that when the system trajectory approaches the sliding-mode surface, the *eq*$(x_1.s)$ gradually decreases to zero to suppress the chattering. Thus, the controller designed by proposed reaching law can dynamically adapt to the variations of the sliding-mode surface and system states $|x_1|$ by making *eq*$(x_1.s)$ vary between k/ε and zero.

Next, according to (10), the reaching time *t* that is the required time for system states to reach *s* can be calculated as

$$\dot{s}\left[\varepsilon + (1+1)/(|x_1| - \varepsilon)e^{-\delta|s|}\right] = -k \cdot \operatorname{sgn}(s). \tag{11}$$

With $s(t) = 0$, integrating (11) from 0 to *t* will yield

$$t = \frac{1}{k}\left[\varepsilon|s(0)| + \frac{(1+1/|x_1| - \varepsilon)}{\delta}(1 - e^{-\delta|s(0)|})\right]. \tag{12}$$

Since $1 - e^{-\delta|s(0)|} < 1$, we can obtain the following inequality:

$$t < \frac{1}{k}\left(\varepsilon|s(0)| + \frac{1+1/|x_1| - \varepsilon}{\delta}\right). \tag{13}$$

Here, if parameter δ is chosen such that $\delta \gg ((1 + 1/|x_1| - \varepsilon)/(\varepsilon|s(0)|))$, and noticing that $x_1 \neq 0$ can always satisfy between 0 and *t*, the inequality (13) can be simplified as follows:

$$t < \frac{\varepsilon|s(0)|}{k}. \tag{14}$$

Therefore, according to (9) and inequality (14), the time difference between *t* and t_1 with the condition that gain $k = k_1$ can be obtained as follows:

$$t - t_1 < \frac{\varepsilon|s(0)|}{k} - \frac{|s(0)|}{k_1} = \frac{|s(0)|}{k}(\varepsilon - 1). \tag{15}$$

Note that the term $|s(0)|/k$ is strictly positive and $\varepsilon - 1$ is always negative, then, inequality (15) implies that $t - t_1 < 0$. This means that novel reaching law improves the reaching speed of the sliding-mode surface with the same gain (i.e., $k = k_1$). On the other hand, if reaching time *t* satisfying $t_1 = t$ is chosen, the following inequality can be obtained:

$$k < \varepsilon k_1. \tag{16}$$

Therefore, it can be guaranteed that the gain *k* less than the gain k_1, which means that the proposed reaching law will reduce the chattering of SMC with the same reaching speed.

Since the reaching law will be only computed at discrete instants and applied to the system during the sampling interval, the discrete form of the proposed reaching law is introduced when the sliding-mode surface is near to 0.

According to the proposed reaching law (10), if sliding-mode surface *s* is near to zero, the denominator term of the $eq(x_1.s)$ approaches $1 + 1/|x_1|$, then the $eq(x_1.s)$ converges to $k|x_1|/(1 + |x_1|)$. Therefore, the proposed reaching law (10) can be simplified as $\dot{s} \approx (-k|x_1|/(1 + |x_1|)) \cdot \operatorname{sgn}(s)$. Its discrete expression is given by

$$s(n+1) - s(n) \approx -\frac{k|x_1|T}{1+|x_1|} \cdot \operatorname{sgn}(s(n)) \tag{17}$$

where $T < 0$ is sampling period. Assume that the system trajectory reaches the sliding-mode surface in a finite time, which implies that $s(n) = 0^+$ or $s(n) = 0^-$, then, the following equation can be obtained in next period with $s(n) = 0^+$:

$$s(n+1) \approx -\frac{k|x_1|T}{1+|x_1|}. \tag{18}$$

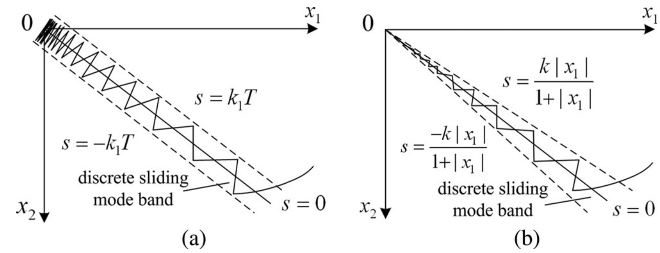

Fig. 1. State trajectories of the equal reaching law and the novel reaching law. (a) Equal reaching law. (b) Novel reaching law.

It can also be written as follows with $s(n) = 0^-$:

$$s(n+1) \approx \frac{k|x_1|T}{1+|x_1|}. \tag{19}$$

Therefore, the width of the discrete sliding-mode band for (17) is

$$\Delta \approx \frac{k|x_1|T}{1+|x_1|}. \tag{20}$$

In the same way, equal reaching law stated in (5) can also be written as follows in discrete form:

$$s_1(n+1) - s_1(n) = -k_1T \cdot \operatorname{sgn}(s_1(n)). \tag{21}$$

Width of the discrete sliding-mode band is

$$\Delta_1 = k_1T. \tag{22}$$

It is obvious that the bandwidth of (22) is a constant. That means the system states under the control of the equal reaching law can not reach the equilibrium point (0, 0), which would generate the chattering phenomena between k_1T and $-k_1T$. However, it can also be found that the bandwidth of (20) decreases with decreasing system state $|x_1|$, which indicates that the system states under the control of the proposed reaching law can reach the equilibrium point (0, 0). Therefore, the chattering of the proposed reaching law is limited effectively, which is a substantial advantage over the conventional SMC. The state trajectories of the equal reaching law and the proposed reaching law are shown in Fig. 1.

B. Speed Controller Design Based on the Proposed Reaching Law

Speed-control algorithms should keep the actual speed track of the speed reference ω_{ref} accurately under the occurrence of disturbances. To achieve this control objective, the tracking error is defined as $e = \omega_{\mathrm{ref}} - \omega$. Then, according to aforementioned sliding-mode design method, the following sliding-mode surface is chosen:

$$S = e = \omega_{\mathrm{ref}} - \omega \tag{23}$$

which is called linear sliding-mode surface. Taking the time derivative of the sliding-mode surface yields

$$\dot{S} = \dot{\omega}_{\mathrm{ref}} - \dot{\omega}. \tag{24}$$

Moreover, according to the (1), the dynamic equation of the motor can be expressed as follows, with the parameters variations taken into accounts:

$$\begin{aligned}\dot{\omega} &= a i_q - b T_L - c\omega \\ &= a_n i_q - b_n T_L - c_n \omega + \Delta a i_q - \Delta b T_L - \Delta c \omega \\ &= a_n i_q - c_n \omega + r(t) \end{aligned} \tag{25}$$

where $a = a_n + \Delta a = 3p^2\psi_a/2J$, $b = b_n + \Delta b = p/J$, and $c = c_n + \Delta c = B/J$. a_n, b_n, and c_n are nominal parameter. Δa, Δb, and Δc are parameter variations. In (25), $r(t) = \Delta a i_q - \Delta c \omega - b T_L$ represents the lumped disturbances including internal parameter variation, friction force, and external load disturbances, which is assumed to be bounded

$$|r(t)| \le l \tag{26}$$

where l is the upper bound of the lumped disturbances.

Furthermore, substituting (25) and the novel reaching law (10) into (24) yields

$$\begin{aligned}\dot{S} &= \dot{\omega}_{\text{ref}} + c_n \omega - r(t) - a_n i_q \\ &= -eq(x_1, S) \cdot \operatorname{sgn}(S). \end{aligned} \tag{27}$$

Therefore, the control input i_q^* is designed as follows:

$$i_q^* = a_n^{-1}\{\dot{\omega}_{\text{ref}} + c_n\omega - r(t) + eq(x_1, S) \cdot \operatorname{sgn}(S)\}. \tag{28}$$

In this control input, the lumped disturbances $r(t)$ is included, which is unknown. Thus, the control input (28) is not yet completive [3]. To deal with this problem, the lumped disturbances $r(t)$ is replaced by the upper bound l, then the following control input is designed:

$$i_q^* = a_n^{-1}\{\dot{\omega}_{\text{ref}} + c_n\omega + [l + eq(x_1, S)] \cdot \operatorname{sgn}(S)\}. \tag{29}$$

From (29), it can be found that upper bound l has an important effect on the control performance. However, it is difficult to select upper bound in practical application, because the lumped disturbances are difficult to know the exact value and measure. Though some methods, such as error control and trial, can be used to select upper bound, these approaches are time consuming and cannot provide enough robustness. Therefore, to overcome this drawback, an SMC with the disturbance compensation method is presented in Section III-D.

C. Simulation and Experimental Results

To demonstrate the effectiveness of the proposed reaching law, simulations, and experiments of sliding-mode speed control using equal reaching law and the proposed reaching law on the PMSM system have been completed and the results are shown in Figs. 2–4. Parameters of PMSM are listed in Table I.

In the simulation and experiment, the disturbances are not considered, i.e., $l = 0$, and the linear sliding-mode surface is chosen (23). The gain of equal reaching law is $k_1 = 20$, and the parameters of the proposed reaching law are: $k = 20$, $\delta = 10$, $\varepsilon = 0.1$, and $x_1 = e$.

The simulation results of the q axes current and switching plane trajectories with speed command $\omega_{\text{ref}} = 500$ r/min are given in Figs. 2 and 3. Meanwhile, the dynamic responses of the motor speed and q axes current are given in Fig. 4(a) and (b) when the speed command is changed from 500 to 1000 r/min.

TABLE I
PARAMETERS OF PMSM

d- and q-axes inductances	$L_d = L_q$ = 11.5mH
Stator phase resistance	r = 3.5Ω
Viscous friction coefficient	B = 0.00001N·m·s/rad
Number of pole pairs	P = 3
Rotational inertia	J = 0.00044kg·m^2
Flux linkage of permanent magnets	ψ_a = 0.107Wb

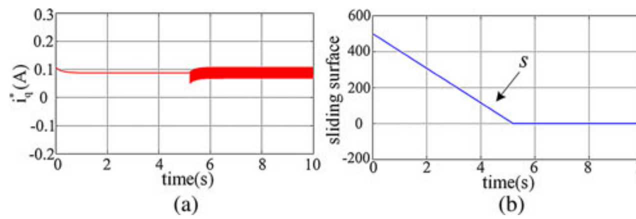

Fig. 2. Simulation results under equal reaching law. (a) q axes current. (b) Switching plane trajectories.

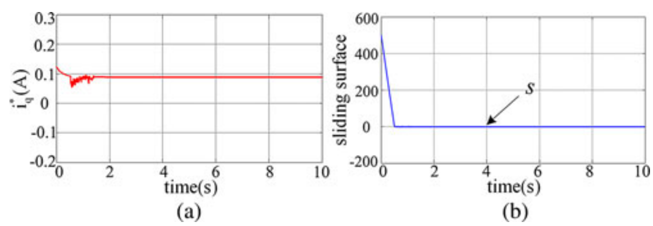

Fig. 3. Simulation results under proposed reaching law. (a) q axes current. (b) Switching plane trajectories.

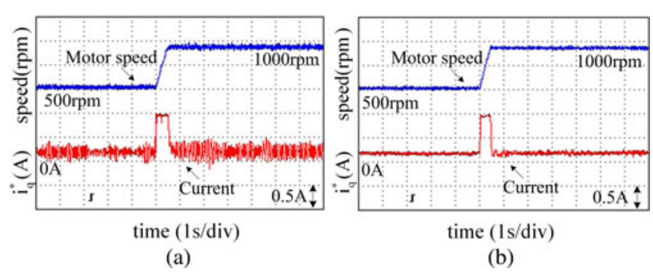

Fig. 4. Performance comparisons under equal reaching law and proposed reaching law (experiment). (a) Equal reaching law. (b) Proposed reaching law.

Simulation and experimental results indicate that the proposed reaching law can reduce the chattering level of SMC system and improve the convergence rate of sliding surface compared with the equal reaching law.

D. ESMDO

The existence of the lumped disturbances will degrade the control performance if the corresponding compensation method is not able to suppress it. To do this, ESMDO is proposed to estimate the lumped disturbances $r(t)$ on line. Then, the estimated disturbances are considered as the feedforward part to compensate the disturbances of aforementioned SMC method stated in (28).

According to (25), also because disturbances $r(t)$ are regarded as the extended system states, an extended dynamic equation can be obtained as

$$\dot{\omega} = a_n i_q - c_n \omega + r(t)$$
$$\dot{r}(t) = d(t) \tag{30}$$

where $d(t)$ is the variation rate of system disturbances $r(t)$.

Then, the ESMDO can be constructed for system (30) as

$$\dot{\hat{\omega}} = a_n i_q - c_n \hat{\omega} + \hat{r}(t) + u_{\mathrm{smo}}$$
$$\dot{\hat{r}}(t) = g u_{\mathrm{smo}} \tag{31}$$

where $\hat{\omega}$ is an estimate of speed ω, $\hat{r}(t)$ is an estimate of lumped disturbances $r(t)$, g is sliding-mode parameter which is discussed in next section, and u_{smo} represents the switching signal that is designed as

$$u_{\mathrm{smo}} = \eta \cdot \mathrm{sgn}(S) \tag{32}$$

where η is negative, and sliding-mode surface S is the same as (23).

Furthermore, the error equation can be obtained as follows by subtracting (30) from (31):

$$\dot{e}_1 = -c_n e_1 + e_2 + u_{\mathrm{smo}}$$
$$\dot{e}_2 = g u_{\mathrm{smo}} - d(t) \tag{33}$$

where $e_1 = \hat{\omega} - \omega$ is speed estimation error, and $e_2 = \hat{r}(t) - r(t)$ is disturbance estimation error.

Based on the error (33) and the reaching condition of sliding mode (2), the ESMDO parameter choice guidelines are introduced as follows.

1) Choice of Observer Parameter: Parameter η should be selected reasonably to ensure sliding mode occurring, which means that the reaching condition (inequality (2)) must be satisfied. Therefore, according to (33) and inequality (2), the reaching condition of sliding mode should be expressed as

$$\begin{aligned} e_1 \cdot \dot{e}_1 &= e_1(-c_n e_1 + e_2 + u_{\mathrm{smo}}) \\ &= e_1[(e_2 - c_n e_1) + \eta \cdot \mathrm{sgn}(e_1)] \\ &= \begin{cases} e_1[(e_2 - c_n e_1) + \eta] < 0 & (e_1 > 0) \\ e_1[(e_2 - c_n e_1) - \eta] < 0 & (e_1 < 0). \end{cases} \end{aligned} \tag{34}$$

As a result,

$$\eta < -|e_2 - c_n e_1|. \tag{35}$$

Thus, in practical application, parameter η should be selected as

$$\eta = -m|e_2 - c_n e_1|, \quad m > 1 \tag{36}$$

where m is safety factor of the sliding mode. Usually, $m = 2$ is enough to ensure the sliding mode exciting.

Therefore, the observer with parameter η stated in (36) can reach sliding-mode surface in a finite time, and stay on it. Then, the following equation can be obtained:

$$e_1 = \dot{e}_1 = 0. \tag{37}$$

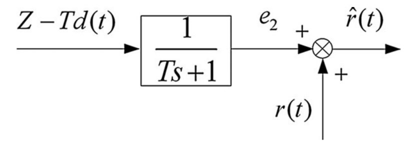

Fig. 5. Chattering suppression structure of the observer

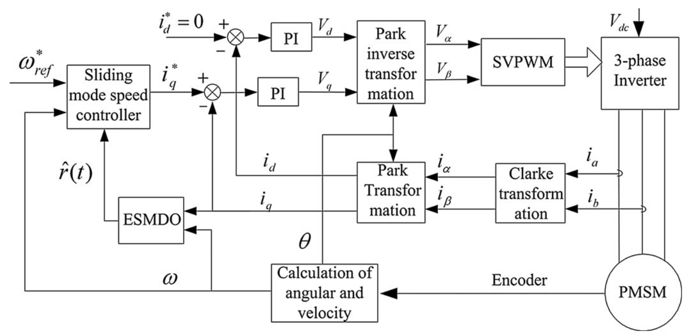

Fig. 6. SMC+ESMDO control scheme of the PMSM speed-regulation system.

Substituting (37) into the error (33) yields

$$e_2 = -u_{\mathrm{smo}}$$
$$\dot{e}_2 = g u_{\mathrm{smo}} - d(t) \tag{38}$$

which can also be rewritten as

$$\dot{e}_2 + g e_2 + d(t) = 0. \tag{39}$$

According to (39), disturbance estimation error is

$$e_2 = e^{-gt}\left[C + \int d(t) \cdot e^{gt} dt\right] \tag{40}$$

where C is a constant. To ensure the disturbance estimation error e_2 converge to zero, the sliding-mode parameter is selected as

$$g > 0. \tag{41}$$

Moreover, the convergence rate of disturbance estimation error is in direct relation with the value of parameter g.

Thus, it can be observed that the choice of the ESMDO parameters is only constrained by relations (36) and (41).

2) Chattering Suppression Analysis: Chattering suppression techniques have already become indispensable in SMC systems. To consider the chattering effect on ESMDO, the first equation of error (38) can be rewritten as

$$e_2 = -u_{\mathrm{smo}} + Z \tag{42}$$

where Z represents the chattering signal. Substituting (42) into the second equation of error (38) yields

$$\dot{e}_2 + g e_2 = gZ - d(t). \tag{43}$$

Let the transfer function of error e_2 be $F(s)$. $F(s)$ is given as follows:

$$F(s) = \frac{e_2}{Z - Td(t)} = \frac{1}{Ts + 1}. \tag{44}$$

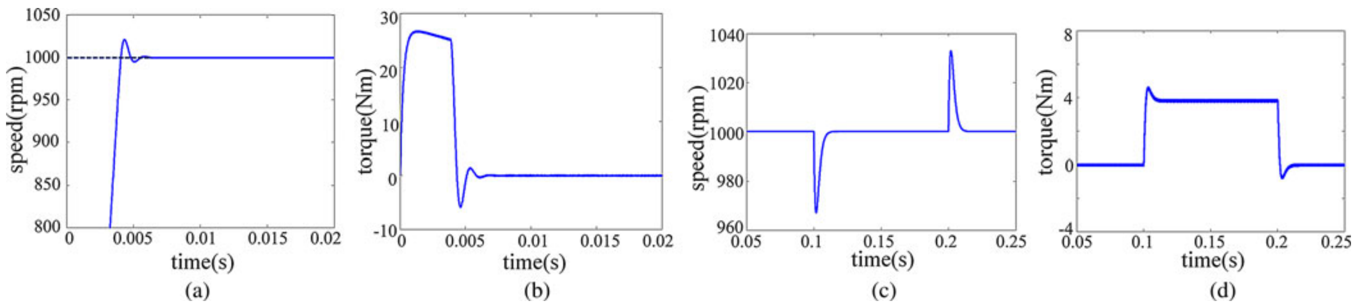

Fig. 7. Simulation results under PI controller. (a) Speed. (b) Torque. (c) Speed in the case of load disturbances. (d) Torque in the case of load disturbances.

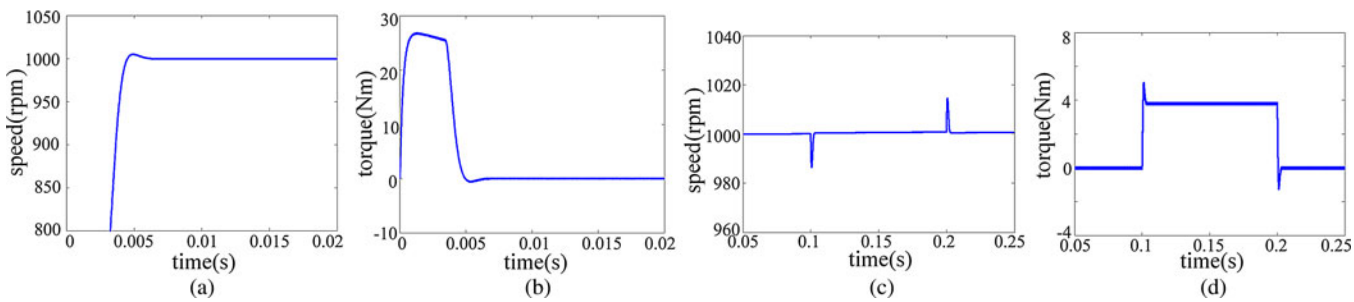

Fig. 8. Simulation results under SMC+ESMDO controller. (a) Speed. (b) Torque. (c) Speed in the case of load disturbances. (d) Torque in the case of load disturbances.

Based on the (44), it can be concluded that $F(s)$ is a low-pass filter (LPF), which can suppress high-frequency signal effectively. The cutoff frequency of LPF is $\omega_c = 1/T = g$. As shown in Fig. 5, chattering signal is suppressed by this LPF.

3) Speed Controller Design Based on the Proposed Reaching Law and ESMDO: To improve the SMC system performance under disturbances, the ESMDO is adopted to estimate disturbances and the SMC+ESMDO approach is developed as shown in Fig. 6. In this approach, estimated lumped disturbances are considered as the feedforward part to compensate disturbances of aforementioned SMC method stated in (28). Thus, the control input i_q^* of the SMC+ESMDO approach is designed as follows:

$$i_q^* = a_n^{-1}\{\dot{\omega}_{\mathrm{ref}} + c_n\omega - \hat{r}(t) + eq(x_1, S)\cdot \mathrm{sgn}(S)\}. \quad (45)$$

In this controller, the system disturbances can be estimated and compensated on line, which will improve the regulation ability of SMC system.

Next, the Lyapunov function $V = S^2/2$ is chosen, and according to (24), (25), and (45), the following relations can be obtained:

$$\begin{aligned}\dot{V} &= S\cdot\dot{S} = S[\dot{\omega}_{\mathrm{ref}} + c_n\omega - r(t) - a_n i_q]\\ &= S[-eq(x_1, S)\cdot \mathrm{sgn}(S)]\\ &= -|S|\, eq(x_1, S) \le 0. \end{aligned} \quad (46)$$

This can guarantee that the designed control system is stable and any tracking error trajectory will converge to zero in a finite time.

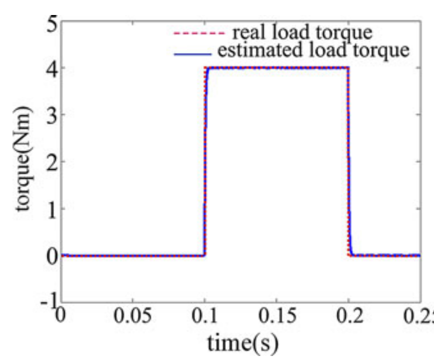

Fig. 9. Estimated load disturbance of the ESMDO (simulation).

E. Simulation and Experimental Results

In this section, to demonstrate the effectiveness of the proposed SMC+ESMDO approach, simulations, and experiments of the PI method and the SMC+ESMDO method in one PMSM system were made. Simulations are established in MATLAB/Simulink, and the experiments platform is constructed by TMS320LF2812 processor.

1) Simulation Results: The PI simulation parameters of the both current loops are the same: the proportional gain $K_{pc} =$ 10, the integral gain $K_{ic} = 2.61$. The PI simulation parameter of the speed loop is that proportional gain $K_{ps} = 0.5$, and integral gain $K_{is} = 20$. The parameters of the SMC+ESMDO speed loop are: $k = 20$, $\delta = 10$, $\varepsilon = 0.1$, and $x_1 = e$.

The simulation results of the PI controller and the SMC+ESMDO controller are shown in Figs. 7 and 8. From the simulation results, it can be observed that the SMC+ESMDO method has a smaller overshoot and a shorter settling time compared with the PI method when the reference speed is

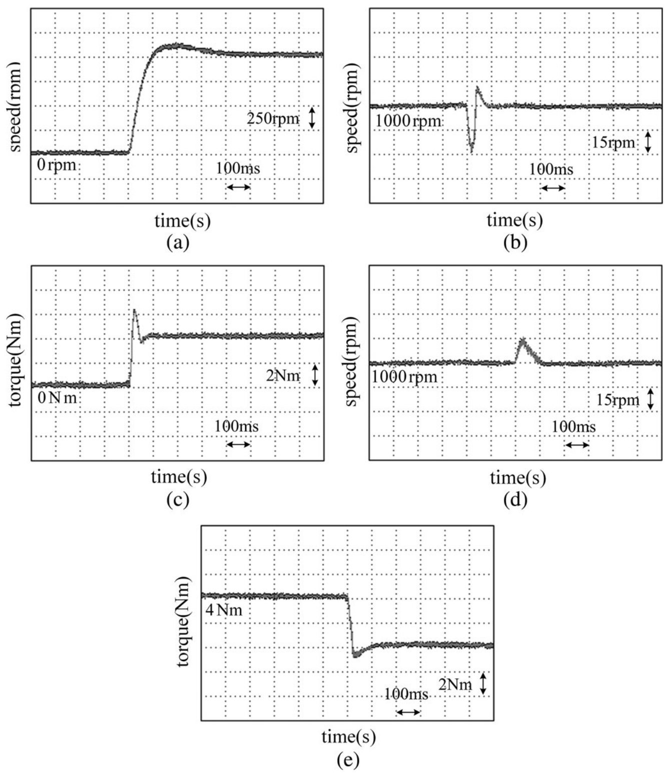

Fig. 10. Experiment results under PI controller. (a) Speed. (b) Speed in the case of sudden load increase. (c) Torque in the case of sudden load increase. (d) Speed in the case of sudden load decrease. (e) Torque in the case of sudden load decrease.

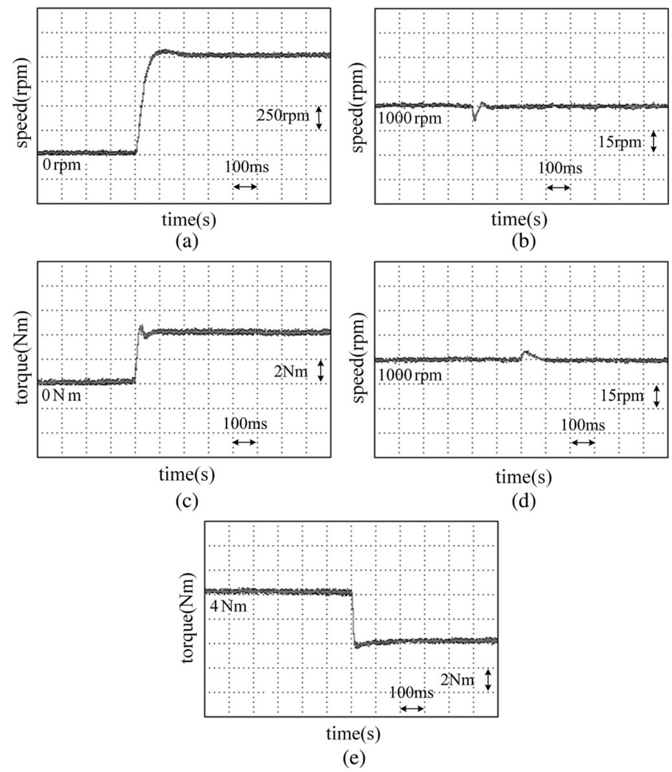

Fig. 11. Experiment results under SMC+ESMDO controller. (a) Speed. (b) Speed in the case of sudden load increase. (c) Torque in the case of sudden load increase. (d) Speed in the case of sudden load decrease. (e) Torque in the case of sudden load decrease.

1000 r/min. Moreover, when load torque $T_L = 4$ N·m is added suddenly at $t = 0.1$ s and removed at $t = 0.2$ s, the SMC+ESMDO method gives less speed and electrical magnetic torque fluctuations. Estimated load disturbance of the ESMDO and load disturbance command are shown in Fig. 9. It can be observed that the ESMDO can estimate the disturbance exactly and quickly with low chattering.

2) Experimental Results: To evaluate the performance of the proposed method, the experimental system for speed control of PMSM was built. The PI parameters of the both current loops are the same: the proportional gain $K_{pc} = 8$, and the integral gain $K_{ic} = 3.3$. The PI parameter of speed loop is that proportional gain $K_{ps} = 1$, and integral gain $K_{is} = 15$. The parameters of SMC+ESMDO speed loop are: $k = 18$, $\delta = 10$, $\varepsilon = 0.2$, and $x_1 = e$.

The experimental results of the PI controller and the SMC+ESMDO controller are shown in Figs. 10 and 11. Figs. 10(a) and 11(a) show the startup procedure of the motor speed when the reference speed is given as 1000 r/min. Moreover, load experiments are carried out, and their performances are compared with each other when the motor is running at a steady state of 1000 r/min. Fig. 10(b), (c), 11(b) and (c) show the dynamic responses of motor speed and torque, when the load torque $T_L = 4$ N·m is added suddenly. On the other hand, when the load torque $T_L = 4$ N·m is removed suddenly, the dynamic responses of motor speed and torque are shown in Figs. 10(d) and (e), 11(d) and (e). Finally, estimated load disturbance of the ESMDO are shown in Fig. 12.

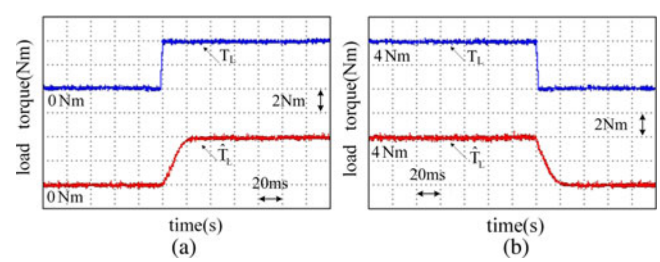

Fig. 12. Estimated load disturbances of the ESMDO (experiment). (a) Load torque command and estimated torque disturbance in case of sudden load increase. (b) Load torque command and estimated torque disturbance in case of sudden load decrease.

From the experimental results, it is obvious that the ESMDO can estimate the disturbance exactly and quickly with low chattering, and the SMC+ESMDO method has satisfying disturbance suppression ability compared with PI method. In practical applications, one can implement the proposed algorithm by following steps. First, an SMC speed controller should be constructed according to the proposed reaching law, and then drives the PMSM. Second, the ESMDO can also be constructed using the (31), then we need to test the effectiveness of the ESMDO when the load is added or removed suddenly. If the disturbance estimate is different from the actual load, one must check whether the parameters of the ESMDO are right. Finally, if the ESMDO can estimate disturbances exactly, estimated disturbances can be considered as the feedforward part to compensate disturbances.

However, it should be noted that the computational complexity of the new method is increased, when compared with the conventional PI method. Specifically, there are four times of multiplications and divisions in antiwindup PI algorithm, while the new algorithm includes nine times of them. Thus, some extra efforts, including a fast data processing capability chip and the accurate disturbances estimate algorithm, are required to implement the proposed method as compared to PI method.

IV. Conclusion

In this paper, one nonlinear SMC algorithm is proposed and has been experimentally applied to a PMSM system, to avoid chattering occurring and to suppress disturbances. The major contributions of this work include: 1) a novel SMRL method is introduced to control the chattering; 2) in order to estimate system disturbances, one extended sliding-mode disturbance observer is presented; and 3) a composite control method that combines SMC and ESMDO is developed to further improve the disturbance rejection ability of SMC system. Simulation and experimental results have validated the proposed method.

References

[1] Y. X. Su, C. H. Zheng, and B. Y. Duan, "Automatic disturbances rejection controller for precise motion control of permanent-magnet synchronous motors," *IEEE Trans. Ind. Electron.*, vol. 52, no. 3, pp. 814–823, Jun. 2005.

[2] X. G. Zhang, K. Zhao, and L. Sun, "A PMSMsliding mode control system based on a novel reaching law," in *Proc. Int. Conf. Electr. Mach. Syst.*, 2011, pp. 1–5.

[3] W. Gao and J. C. Hung, "Variable structure control of nonlinear systems: A new approach," *IEEE Trans. Ind. Electron.*, vol. 40, no. 1, pp. 45–55, Feb. 1993.

[4] G. Feng, Y. F. Liu, and L. P. Huang, "A new robust algorithm to improve the dynamic performance on the speed control of induction motor drive," *IEEE Trans. Power Electron.*, vol. 19, no. 6, pp. 1614–1627, Nov. 2004.

[5] Y. A.-R. I. Mohamed, "Design and implementation of a robust current-control scheme for a pmsm vector drive with a simple adaptive disturbance observer," *IEEE Trans. Ind. Electron.*, vol. 54, no. 4, pp. 1981–1988, Aug. 2007.

[6] M. A. Fnaiech, F. Betin, G.-A. Capolino, and F. Fnaiech, "Fuzzy logic and sliding-mode controls applied to six-phase induction machine with open phases," *IEEE Trans. Ind. Electron.*, vol. 57, no. 1, pp. 354–364, Jan. 2010.

[7] Y. Feng, J. F. Zheng, X. H. Yu, and N. Vu Truong, "Hybrid terminal sliding mode observer design method for a permanent magnet synchronous motor control system," *IEEE Trans. Ind. Electron.*, vol. 56, no. 9, pp. 3424–3431, Sep. 2009.

[8] H. H. Choi, N. T.-T. Vu, and J.-W. Jung, "Digital implementation of an adaptive speed regulator for a pmsm," *IEEE Trans. Power Electron.*, vol. 26, no. 1, pp. 3–8, Jan. 2011.

[9] R. J. Wai and H. H. Chang, "Backstepping wavelet neural network control for indirect field-oriented induction motor drive," *IEEE Trans. Neural Netw.*, vol. 15, no. 2, pp. 367–382, Mar. 2004.

[10] G. H. B. Foo and M. F. Rahman, "Direct torque control of an ipm-synchronous motor drive at very low speed using a sliding-mode stator flux observer," *IEEE Trans. Power Electron.*, vol. 25, no. 4, pp. 933–942, Apr. 2010.

[11] D. W. Zhi, L. Xu, and B. W. Williams, "Model-based predictive direct power control of doubly fed induction generators," *IEEE Trans. Power Electron.*, vol. 25, no. 2, pp. 341–351, Feb. 2010.

[12] K. Zhao, X. G. Zhang, L. Sun, and C. Cheng, "Slidingmode control of high-speed PMSM based on precision linearization control," in *Proc. Int. Conf. Electr. Mach. Syst.*, 2011, pp. 1–4.

[13] C.-S. Chen, "Tsk-type self-organizing recurrent-neural-fuzzy control of linear microstepping motor drives," *IEEE Trans. Power Electron.*, vol. 25, no. 9, pp. 2253–2265, Sep. 2010.

[14] M. Singh and A. Chandra, "Application of adaptive network-based fuzzy inference system for sensorless control of PMSG-based wind turbine with nonlinear-load-compensation capabilities," *IEEE Trans. Power Electron.*, vol. 26, no. 1, pp. 165–175, Jan. 2011.

[15] L. Wang, T. Chai, and L. Zhai, "Neural-network-based terminal sliding-mode control of robotic manipulators including actuator dynamics," *IEEE Trans. Ind. Electron.*, vol. 56, no. 9, pp. 3296–3304, Sep. 2009.

[16] J. Y.-C. Chiu, K. K.-S. Leung, and H. S.-H. Chung, "High-order switching surface in boundary control of inverters," *IEEE Trans. Power Electron.*, vol. 22, no. 5, pp. 1753–1765, Sep. 2007.

[17] B. Castillo-Toledo, S. Di Gennaro, A. G. Loukianov, and J. Rivera, "Hybrid control of induction motors via sampled closed representations," *IEEE Trans. Ind. Electron.*, vol. 55, no. 10, pp. 3758–3771, Oct. 2008.

[18] F. J. Lin, J. C. Hwang, P. H. Chou, and Y. C. Hung, "FPGA-based intelligent-complementary sliding-mode control for pmlsm servo-drive system," *IEEE Trans. Power Electron.*, vol. 25, no. 10, pp. 2573–2587, Oct. 2010.

[19] C. J. Fallaha, M. Saad, H. Y. Kanaan, and K. Al-Haddad, "Sliding-mode robot control with exponential reaching law," *IEEE Trans. Ind. Electron.*, vol. 58, no. 2, pp. 600–610, Feb. 2011.

[20] S. Li and Z. Liu, "Adaptive speed control for permanent magnet synchronous motor system with variations of load inertia," *IEEE Trans. Ind. Electron.*, vol. 56, no. 8, pp. 3050–3059, Aug. 2009.

Xiaoguang Zhang was born in Heilongjiang, China, in 1985. He received the B.S. degree in electrical engineering from the Heilongjiang Institute of Technology, Harbin, China, in 2007, and the M.S. degree in electrical engineering from the Harbin Institute of Technology, Harbin, in 2009, where he is currently working toward the Ph.D. degree in electrical engineering.

His research interests include electric machines and drives, and power electronics.

Lizhi Sun (M'08–SM'08) received the B.S. degree from the Harbin University of Science and Technology, Harbin, China, in 1993, and the M.S. and Ph.D. degrees in electrical engineering from the Harbin Institute of Technology, in 1995 and 1998, respectively.

He is currently a Professor at the Harbin Institute of Technology. From 2007 to 2008, he was a Research Associate at Wisconsin Electric Machines and Power Electronics Consortium, University of Wisconsin–Madison, Madison. His research interests include electric machines and drives.

Ke Zhao was born in Harbin, China, in 1973. He received the B.S. degree in electrical engineering from the Harbin University of Science and Technology, Harbin, in 1996, and the M.S. and Ph.D. degrees in electrical engineering from the Harbin Institute of Technology, in 2002 and 2008, respectively.

He is currently a Lecturer of Electrical Machine and Apparatus, Harbin Institute of Technology. His research interests include electric machines and drives, and wind-power generation system.

Li Sun (M'08) was born in Heilongjiang, China, in 1960. He received the B.S., M.S., and Ph.D. degrees in electrical engineering from the Harbin Institute of Technology, Harbin, China, in 1982, 1986, and 1991, respectively.

Since 1986, he has been in the Department of Electrical Engineering, Harbin Institute of Technology, where he is currently a Professor and a Doctor Supervisor of Electrical Machine and Apparatus. His research interests include electric machines and drives, power electronics and applications, and electromagnetic compatibility.